THE EFFECT OF SiC PARTICLES VOLUME FRACTION ON HOT DEFORMATION BEHAVIOR OF AA 2024 COMPOSITES REINFORCED WITH SiC PARTICLES

Byung-Chul Ko and Yeon-Chul Yoo

Department of Metallurgical Engineering, Inha University, Inchon 402-751, Korea

ABSTRACT Hot torsion tests were conducted to investigate the hot deformation behavior of AA 2024 composites reinforced with different volume fractions (5, 10, 15, 20, and 30 vol. %) of SiC_p reinforcements. Hot restoration, dynamic recrystallization (DRX) and dynamic recovery (DRV) of the composites were studied from the flow curves and deformed microstructures. The matrix grain size and dislocation density of the composites were investigated by transmission electron microscopy. The effect of SiC_p volume fraction on the critical strain for onset of DRX was analyzed from the relationship between the work hardening rate and effective strain. DRX was occurred in all the composites during hot deformation at 370 - 430 ℃ under a strain rate of 1.0/sec. Also, the flow stress and the dislocation density of the composites increased with increasing volume fraction of SiC_p and also the difference in flow stresses of the composites reinforced with 15, 20, and 30 vol. % of SiC_p deformed at 370 ℃ was small.

Keywords: *hot restoration, dynamic recrystallization, work hardening rate, critical strain, dislocation density, flow stress*

1. INTRODUCTION

The SiC_p reinforcements in the composites increase the hot-strength of the composites and reduce the hot workability because they increase the initial high dislocation density caused by the difference in thermal expansion coefficient (ΔCTE) of the matrix and reinforcements and by the constraints of plastic flow arising from their relative rigidity during hot deformation [1, 2, 3].

Many workers have reported the hot deformation behavior of the Al-based composites reinforced with discontinuous reinforcements of particles or whiskers is quite different from that of the unreinforced monolithic alloy [4-9]. For example, the reinforcement in the composites contributes to a development of small equiaxed substructure compared to the unreinforced monolithic alloy [3]. Also, the addition of SiC whisker (SiC_w) into the AA 2124 matrix alloy promotes the dynamic recrystallization by increasing the dislocation density during hot deformation [4]. In this study, we investigated the hot restoration, flow stress and flow strain of the AA 2024 composites reinforced with various SiC_p volume fractions by torsion tests.

2. EXPERIMENTAL

To investigate the hot deformation behavior of AA 2024 composites reinforced with different volume fractions of SiC_p (5, 10, 15, 20, and 30 vol. %), the composites were fabricated by powder metallurgy route. The materials used in this work are SiC_p reinforcements (~8 ㎛) and AA2024 alloy powders (~44 ㎛ diameter). For the fabrication of the composites, the Al powders and SiC_p were ball-milled for 72 hours and the resulting mixtures were compacted by hot-pressing at 520 ℃ and 120 MPa in vacuum before cooling. The hot-pressed billets with a diameter of 50 ㎜ and a length of 50 ㎜ were hot-extruded with an extrusion ratio of 25 : 1 at 430 ℃. The torsion specimens with a gauge length of 10 mm and a diameter of 7 mm were machined from the extruded composites bars. The samples for torsion tests were heated up to 320 - 500 ℃ using a dual elliptical radiant furnace and then kept for 10 min. Torsion tests were conducted under a strain rate of 1.0/sec. Subsequently, the torsion-tested specimens were quenched immediately into the water at 25 ℃. The effective stress (σ) and effective strain (ε) of the composites were calculated by the von Mises criterion [10] using the torque moment (M) and angular displacement ($\theta = 2\pi rN/L$) measured from the torsion tests. The following equations were used for surface strains and related stresses:

$$\sigma = \sqrt{3}\, M(3+m+n)/2\pi r^3$$
$$\varepsilon = 2\pi rN/\sqrt{3}L$$

where, r is the gauge radius, N is the twist number, L is the gauge length, M is the torque moment, m is the strain rate sensitivity, and n is the strain hardening exponent.

Transmission electron microscopy (TEM) was used to examine the microstructures of hot deformed composites. The specimens for TEM observation were sectioned perpendicular to the extrusion axis. The TEM specimens were mechanically ground to ~60 μm and then jet-polished with a solution of 25 % nitric acid and 75 % methanol under a condition of 30 V and 60 mA at about -40 ℃.

3. RESULTS AND DISCUSSION

The flow curves of the composites and monolithic AA 2024 alloy deformed at 370 and 430 ℃ are shown in Figure 1. In Figure 1(a), as the volume fraction of SiCp increases, the flow stress of the composites increases and the failure strain decreases. The composite reinforced with 30 vol. % SiCp exhibits the highest flow stress (~171.1 MPa) at 370 ℃. The flow stress (~116.2 MPa) of the AA 2024 monolithic alloy is lower than that of the composites but the failure strain (~22.1) is much higher than that of the composites. Also, it was found that at 370 ℃, the difference in flow stresses between the composites reinforced with 20 and 30 vol. % SiCp become small and the flow curves display much higher work hardening behavior than the other composites and monolithic AA 2024 alloy.

In Figure 1(b), the composites and monolithic AA 2024 alloy deformed at 430 ℃ exhibit a lower work hardening behavior than that deformed at 370 ℃. The work hardening of the composite with 5 vol. % SiCp is similar to that of the monolithic AA 2024 alloy. It is also found that at 430 ℃, flow stresses of the composites reinforced with 15, 20, and 30 vol. % SiCp are similar. Therefore, with increasing deformation temperature from 370 to 430 ℃, the critical volume fraction of SiCp, contributing to a strengthening of the composites, decreases from 20 to 15 vol. %. This result implies that at high temperature of 480 ℃, difference in flow stresses between the composites and monolithic alloy is small and there would be little SiCp strengthening at above 480 ℃.

Table 1 is the critical strain (ε_c) for onset of DRX of the composites deformed at various temperatures. The ε_c for DRX of the composites is calculated from the relationship between the work hardening rate and effective strain using a flow curves shown in Figure 1 [11]. The composite reinforced with 20 vol. % SiCp showed the highest work hardening rate. It is also found that the ε_c of the composites deformed at 430 ℃ is smaller than that at 370 ℃.This indicates that with increasing deformation temperature, the work hardening rate of the composites decreases because of an increase in grain size and a decrease in dislocation density of the matrix and also the ε_c for

DRX of the composites is significantly influenced by SiCp volume fraction and deformation temperature.

As shown in Table 1, the values of ε_c of the composite reinforced with 20 vol. % SiCp deformed at 320, 370, 430, 480, and 500 ℃ were ~0.075, ~0.070, ~0.063, ~0.062, and ~0.058, respectively. These values are quite similar to those of the composite reinforced with 30 vol. % SiCp and are lower than those of other composites. These results suggest that the composite with 20 vol. % SiCp is the most effective for the nucleation of DRX at an earlier strain stage during hot deformation. This is because, even though the SiCp reinforcements in the composite are non-uniformly distributed, the matrix grains of the composite are smaller and the dislocation density of the matrix is higher relative to the other composites and monolithic AA 2024 matrix alloy. As the volume fraction of SiCp increases, the degree of SiCp clustering increases, leading to a decrease in ability of load transfer from the matrix to the SiCp during hot deformation. Therefore, the composite with 30 vol. % SiCp may give rise to a lower work hardening rate than the composite with 20 vol. % SiCp.

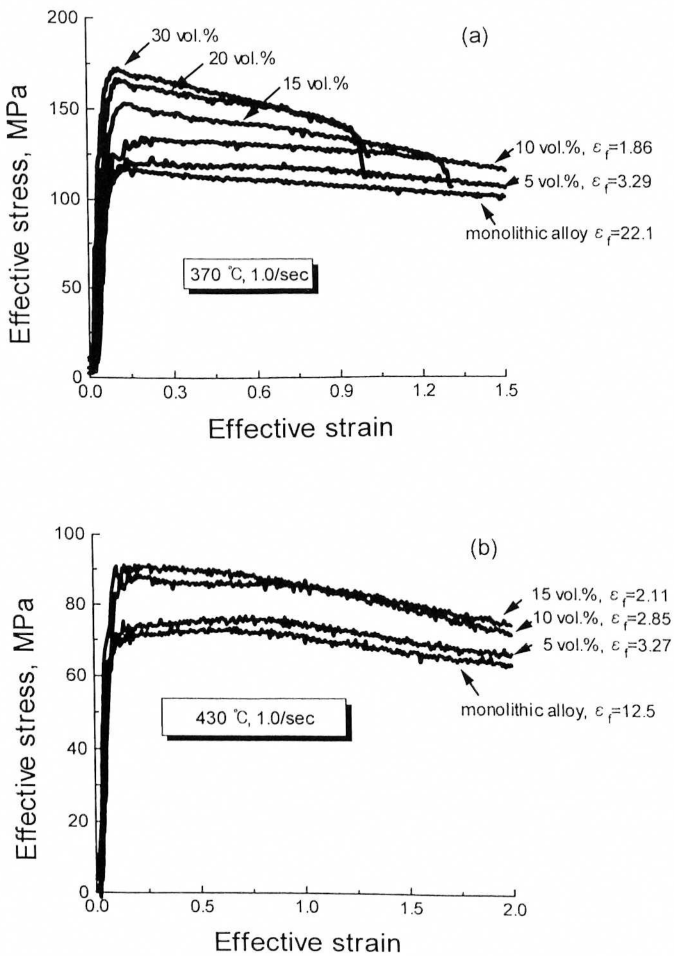

Fig. 1. The stress-strain curves of the SiCp/AA 2024 composites and monolithic AA 2024 alloy deformed at (a) 370 and (b) 430 ℃ under a strain rate of 1.0/sec.

Table 1. Critical and peak strains for DRX of the AA 2024 composites reinforced with different volume fraction of SiCp and monolithic AA 2024 alloy deformed at various temperatures under a strain rate of 1.0/sec.

Temp. (℃)	Critical strain (ε c)						Peak strain (ε p)					
	Monolithic alloy	5 vol. %	10 vol. %	15 vol. %	20 vol. %	30 vol. %	Monolithic alloy	5 vol. %	10 vol. %	15 vol. %	20 vol. %	30 vol. %
320	0.123	0.112	0.090	0.078	0.075	**0.071**	0.158	0.153	0.171	0.113	**0.173**	0.149
370	0.121	0.110	0.089	0.071	**0.070**	0.070	0.149	0.139	**0.169**	0.101	0.126	0.144
430	0.115	0.108	0.085	0.065	**0.063**	0.064	0.144	0.120	**0.165**	0.092	0.124	0.140
480	0.094	0.089	0.074	0.063	**0.062**	0.062	0.115	0.109	**0.140**	0.091	0.122	0.120
500	-	-	0.066	0.055	**0.058**	0.059	-	-	0.110	0.075	**0.122**	0.113

Figure 2 is the TEM bright field images of the AA2024 composites deformed at 370 ℃. The dislocation density of the composites increased with increasing the volume fraction of SiCp and decreasing the deformation temperature.

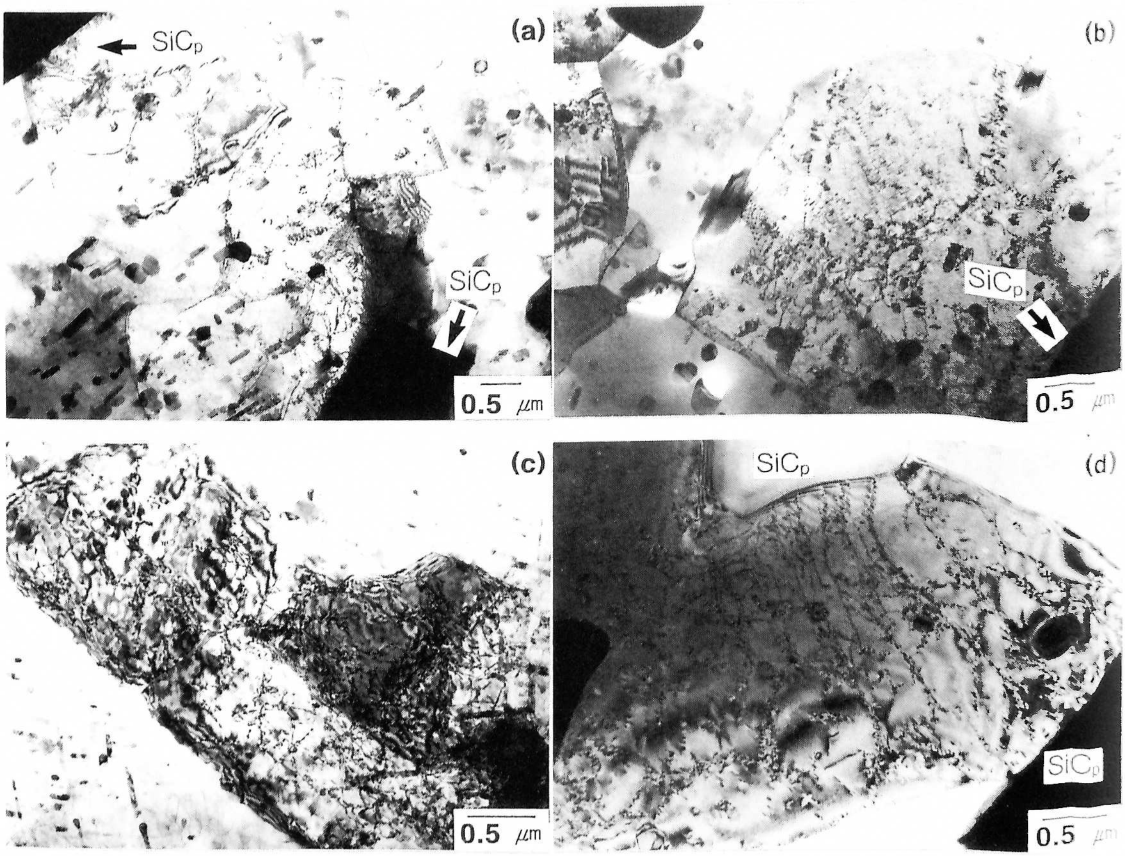

Fig. 2. TEM bright field images of the AA 2024 composites reinforced with (a) 5, (b) 10, and (c) 15 vol. % SiCp deformed at 370 ℃. (d) TEM bright field image of the AA 2024 composite reinforced with 15 vol. % SiCp deformed at 480 ℃.

The AA2024 composite with 20 vol. % SiCp presents small equiaxed grains with dislocation substructure. The average grain size of the composites after hot deformation decreased with increasing the volume fraction of SiCp. The DRX grains are predominantly observed around the SiCp. The high dislocation density around the SiCp can promote the DRX nucleation during hot deformation. Therefore, the ε_c for DRX of the composites was smaller than that of the monolithic AA 2024 alloy.

The dynamic recrystallized grains could be confirmed by TEM investigation. Figure 3(a) shows the TEM bright field image of the dynamic recrystallized grains of the composite with 5 vol. % SiCp. The selected area diffraction (SAD) patterns obtained from the subgrains marked by V, W, and X in Figure 3(a) are shown in Figures 3(b), (c), and (d), respectively, confirming that the DRX occurred during hot deformation. Also, the subgrain marked by X in Figure 3(a) are highly misoriented with neighboring grains (Y and Z in Figure 3(a)). Figures 3(e) and (f) show the SAD patterns from the grains indicated by Y and Z shown in Figure 3(a), respectively.

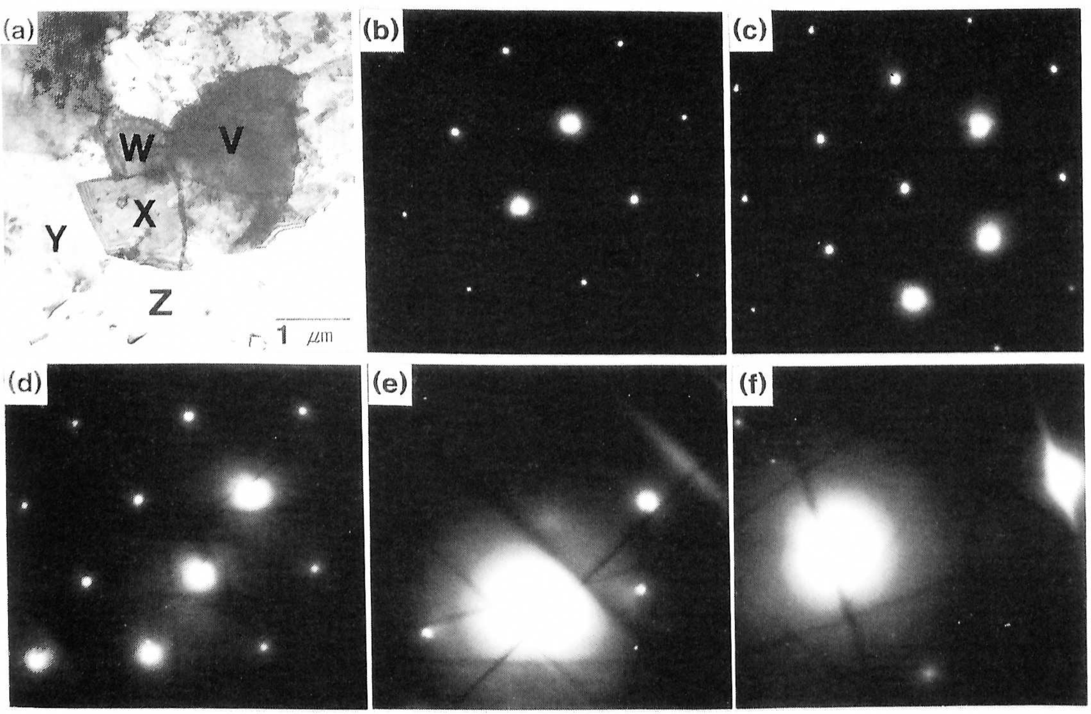

Fig. 3(a) TEM bright image of the dynamic recrystallized grains in the AA 2024 composite with 5 vol. % SiCp deformed at 370 ℃. SAD patterns obtained from the subgrains marked by (b) V, (c) W, and (d) Z in (a). Note small misorientation between V, W, and Z subgrains in (a). SAD patterns obtained from the grains indicated by (e) Y and (f) Z in (a).

4. CONCLUSIONS

For 370 ℃ deformation temperature, the DRX was responsible for the hot restoration of the AA 2024 composites reinforced with SiCp and also the flow stresses of the composites with 20 and 30 vol. % SiCp were similar each other but and were higher than those of other composites. The highest work hardening rate was obtained in the composite with 20 vol. % SiCp. For 370-480 ℃ deformation temperature, the critical strain for onset of DRX of the composites decreased with increasing volume fraction of SiCp except for the composite with 30 vol. % SiCp. As the volume fraction of SiCp increases, the degree of SiCp clustering in the matrix increased, resulting in a decrease in ability of load transfer from the matrix to the reinforcement during hot deformation. Therefore, the critical strain of the composite with 20 vol. % SiCp was similar to that of the composite with 30 vol. % SiCp.

ACKNOWLEDGMENT

This work was supported by Korea Ministry of Education Research Fund for Advanced Materials in 1997.

REFERENCES

[1] D. C. Dunand and A. Mortensen: Acta metall. mater., **39**(7), (1991), 1417.
[2] M. Vogelsang, R. J. Arsenault, and R. M. Fisher: Metall. Trans., **17A**, (1986), 379.
[3] X. Xia, P. Sakaris, and H. J. McQueen: Mater. Sci. and Technol., **10**, (1994), 487.
[4] Y. C. Yoo, J. S. Jeon, and H. I. Lee: Comp. Sci. and Technol., **57**, (1997), 651.
[5] B. C. Ko and Y. C. Yoo: Comp. Sci. and Technol., in press.
[6] B. C. Ko, K. Park, and Y. C. Yoo: Mater. Sci. and Technol., in press.
[7] G. Gonzalez-Doncel and O. D. Sherby: Acta Metall. Mater., **41**(10), (1993), 2797.
[8] F. J. Humphreys, W. S. Miller, and M. R. Djazeb: Mater. Sci. and Technol., **6**, (1994), 1157.
[9] S. I. Hong, G. T. Gray III and J. J. Lewandowski: Acta Metall. Mater., **41**(8), (1993), 2337.
[10] K. Mills, J. R. Davis, J. D. Destefani, D. A. Dieterich, G. M. Crankovic, H. J. Frissel, D. M. Jenkins, W. H. Cubberly, and R. L. Stedfeld: 'Metals Handbook: Mechanical Testing', **8**, (1985), 154; ASM, Metals Park, OH.
[11] N. D. Ryan and H. J. McQueen: High Temp. Technol., **8**(1), (1990), 27.